ROM SAF Report 38
Ref: SAF/ROM/METO/REP/RSR/038
Web: www.romsaf.org
Date: 19 Aug 2020

EUMETSAT
ROM SAF
RADIO OCCULTATION METEOROLOGY

ROM SAF Report 38

An initial assessment of the quality of RO data from COSMIC-2

N E Bowler

Met Office, Exeter, UK

Document Author Table

	Name	Function	Date	Comments
Prepared by:	N E Bowler	ROM SAF Project Team	19 Aug 2020	
Reviewed by:	J Eyre	Met Office review	24 Apr 2020	
Approved by:	K B Lauritsen	ROM SAF Project Manager	17 Aug 2020	

Document Change Record

Issue/Revision	Date	By	Description
0.1	21 Feb 2020	NEB	1st draft
0.2	01 May 2020	NEB	2nd draft, following John's review
1.0	17 Aug 2020	NEB	Final version, following review by KBL

ROM SAF

The Radio Occultation Meteorology Satellite Application Facility (ROM SAF) is a decentralised processing centre under EUMETSAT which is responsible for operational processing of radio occultation (RO) data from the Metop and Metop-SG satellites and radio occultation data from other missions. The ROM SAF delivers bending angle, refractivity, temperature, pressure, humidity, and other geophysical variables in near real-time for NWP users, as well as reprocessed Climate Data Records (CDRs) and Interim Climate Data Records (ICDRs) for users requiring a higher degree of homogeneity of the RO data sets. The CDRs and ICDRs are further processed into globally gridded monthly-mean data for use in climate monitoring and climate science applications.
The ROM SAF also maintains the Radio Occultation Processing Package (ROPP) which contains software modules that aid users wishing to process, quality-control and assimilate radio occultation data from any radio occultation mission into NWP and other models.
The ROM SAF Leading Entity is the Danish Meteorological Institute (DMI), with Cooperating Entities: i) European Centre for Medium-Range Weather Forecasts (ECMWF) in Reading, United Kingdom, ii) Institut D'Estudis Espacials de Catalunya (IEEC) in Barcelona, Spain, and iii) Met Office in Exeter, United Kingdom. To get access to our products or to read more about the ROM SAF please go to: https://www.romsaf.org

Intellectual Property Rights

Abstract

The COSMIC-2 / FORMOSAT-7 constellation of six satellites were launched in June 2019 into low-inclination orbits. These provide radio-occultation observations that are principally focussed on the tropical region. Each satellite carries a TGRS receiver that can make observations from both the GPS and GLONASS GNSS networks.

The constellation provides a substantial increase in the total amount of radio occultation data available, with between 5000 and 6000 per day being expected to be provided. This is more than a 100% increase on the current operational network. The observations are generally of good quality and comparable to observations from the Metop satellites. There are some differences between the COSMIC-2 and Metop constellations, with some indications that COSMIC-2 is performing better in the troposphere. The design of the TGRS receiver gives a higher signal-to-noise ratio compared to other receivers with the hope that this will improve the performance in lower regions of the atmosphere.

Assimilation of these observations indicates that there are substantial benefits from assimilating these data, particularly to NWP forecast performance in the tropics. This study has been focussed on offline data that have been provided. These observations have recently become available in near-real time on the Global Telecommunications System (GTS). Therefore operational assimilation of these data is something that is being actively investigated.

Contents

1 Bending angle evaluation

In April 2006 a constellation of six satellites for making radio-occultation measurements was launched. This constellation was called COSMIC-1 (Constellation Observing System for Meteorology, Ionosphere and Climate) / FORMOSAT-3 (FORMOsa SATellite) and was jointly funded by the USA and Taiwan. It brought a large increase in the number of radio-occultation observations available for Numercial Weather Prediction (NWP) and for studies of the climate. As a follow-up the COSMIC-2 / FORMOSAT-7 constellation of six satellites was launched in June 2019 into low-inclination orbits.

The data being assessed are for the months October 2019 to January 2020 (inclusive). During this time the satellites were undergoing testing and validation. Therefore data from all satellites are not available at all times. Additionally the satellites are in the process of spreading apart from each other. They all began in an orbit at approximately 720 km altitude, and are descending one-by-one to approximately 550 km altitude.

1.1 Bias and standard deviation characteristics

Figure 1.1 shows the normalised difference between the bending angle observation and the background forecast from the Met Office's operational global numerical weather prediction (NWP) model for observations in the tropics (+/- 20 degrees). These differences are known as the innovations. The mean and standard deviation are calculated as

$$\mu = \frac{1}{N}\sum_{i=1}^{N}\frac{O_i - B_i}{B_i} \tag{1.1}$$

$$\sigma = \sqrt{\frac{1}{N}\sum_{i=1}^{N}\left(\frac{O_i - B_i}{B_i} - \mu\right)^2} \tag{1.2}$$

where O_i and B_i are the observed and background values for occultation i in the period, and there are N occultations overall. Figure 1.1 compares the statistics of all the COSMIC-2 satellites with all the Metop satellites. The data have been restricted to near the equator (+/- 20 degrees) in order to create a dataset that is directly comparable. COSMIC-2 provides many more observations in this region, partly due to the latiduinal restriction. Each satellite is able to make observations from both the GPS and GLONASS satellite constellations, meaning that they are able to make many more observations than each Metop satellite (which can only receive GPS signals).

It will be noticed that there is a reduction in the number of observations around 18 km impact altitude. This reduction is related to the Met Office's quality control, since one of the quality control steps is a check on the difference between the observed value and the optimised 1D-Var solution. Since the observations are very variable in this vertical region of the tropics, the quality control erroneously flags many of these observations as having gross errors.

The mean normalised innovation is rather similar between COSMIC-2 and Metop satellites. The principal difference between these are the behaviour in the troposphere, where Metop has a known bias, and above 50 km altitude. To explore this latter difference in more detail, Figure 1.2 shows the mean innovation, averaged between 55 and 60 km altitude. In the region north of the equator, the mean innovation for COSMIC-2 is more positive, and the region of near-zero average innovations is absent. It is difficult to know whether the behaviour of the Metop or COSMIC-2 observations in this

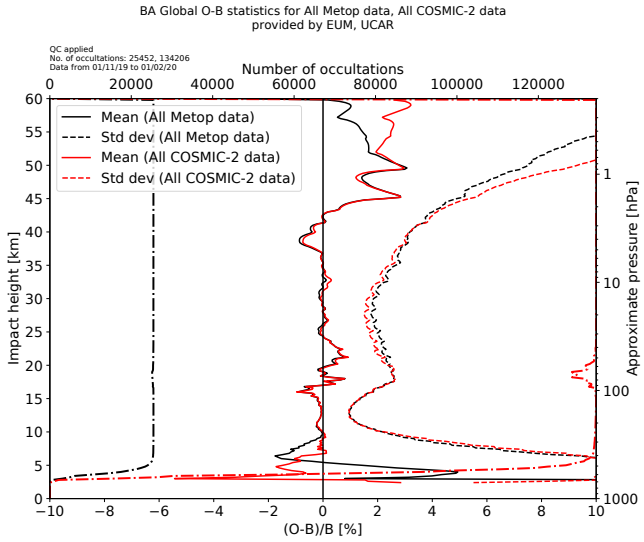

Figure 1.1: The bias and standard deviation of the normalised difference between the observation and the NWP model background forecast $(O-B)/B$ for bending angle. Statistics for all COSMIC-2 observations are compared against observations from Metop. Both sets of data are restricted to the latitude range +/- 20 degrees.

region better reflects the true state of the atmosphere, since there are few independent observations in this region. Another difference of interest is the mean innovation in the lower stratosphere (17 to 20 km altitude). Figure 1.3 shows the mean innovation in this region. Outside the tropics (+/- 30 degrees) the mean innovation for Metop is strongly negative. There is little evidence of similar behaviour in the observations from COSMIC-2, especially over the south Atlantic and Indian oceans where the mean innovation for COSMIC-2 is strongly positive. There is general agreement around the strong negative among other satellites, so this may indicate a region where COSMIC-2 observations are an outlier.

The standard deviation of the normalised innovations (Figure 1.1) shows smaller standard deviations for COSMIC-2 between 20 and 40 km, and smaller standard deviations Metop above this. The lower standard deviation for COSMIC-2 in the region 20 to 40 km may be related to the verti-

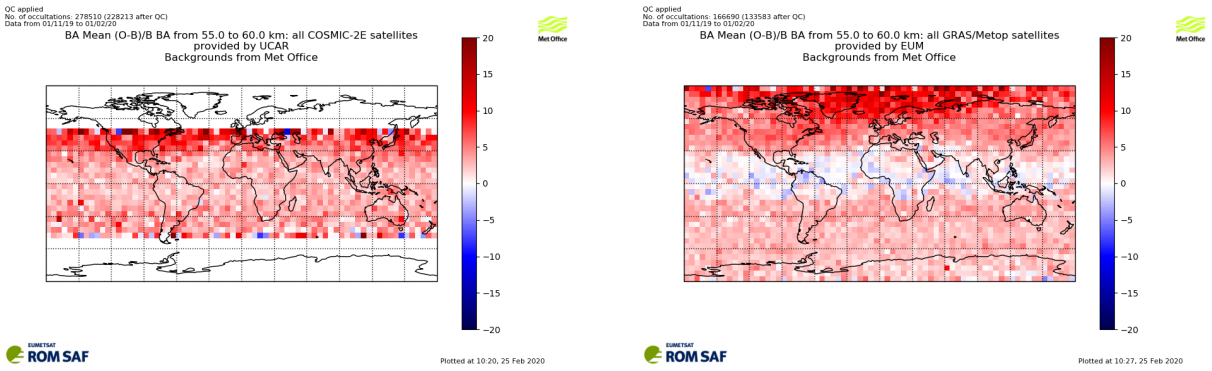

Figure 1.2: Spatial distribution of the mean normalised innovation for bending angles between 55 and 60 km impact altitude.

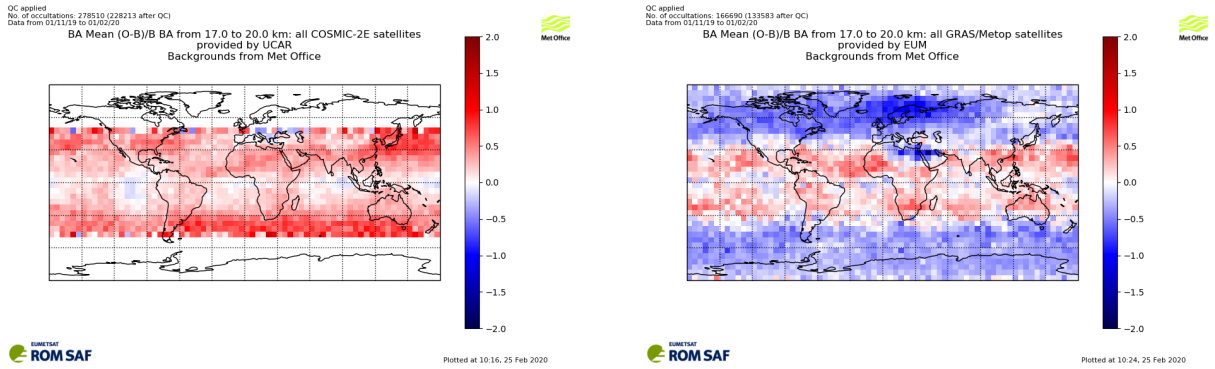

Figure 1.3: Spatial distribution of the mean normalised innovation for bending angles between 17 and 20 km impact altitude.

cal smoothing applied to the data, which then affects the vertical correlations. The systems onboard Metop are particularly accurate at high altitude due to the accuracy of the onboard clock and other processing systems. Thus the standard deviations for Metop are smaller than those for COSMIC-2 above 40 km, in spite of the receiver on COSMIC-2 having a higher signal-to-noise ratio.

Given that COSMIC-2 can receive signals from both GPS and GLONASS, it is instructive to compare the observations made using both constellations. Figure 1.4 shows many more GPS observations are being made than with GLONASS. The mean and standard deviation of the innovations are very similar, except that the standard deviation of the innovations for GLONASS are larger above 35 km. This is consistent with the results shown in Figure 5 of [2].

1.2 Vertical correlations

When bending angle observations are assimilated into the Met Office's NWP system it is assumed that the error in each bending angle measurement is independent of the errors in every other measurement. Therefore we would like the vertical observation-error covariance matrix $\mathbf{R}$ to be diagonal, and the vertical correlations of $O-B$ (which corresponds to the covariance matrix $\mathbf{B}+\mathbf{R}$) to be close to diagonal, containing only the correlations from the background-error covariance matrix. Figure 1.5 shows the vertical correlation of the normalised innovations for data from COSMIC-2 and from the Metop satellites. Due to the way that bending angle is calculated as a smoothed difference between Doppler shifts, we expect a region of positive correlations near the diagonal, and negative correlations at further distances.

Above 20 km impact altitude the vertical correlations for COSMIC-2 are longer range than those from the Metop satellites. Between 10 and 20 km the two sets of vertical correlations have a similar shape to each other. Below 10 km the vertical correlations for COSMIC-2 retain the structure of a core of positive correlations surrounded by a thin region of negative correlations, whereas the vertical correlations for the Metop satellites become somewhat broader and do not have the region of negative correlations. These negative correlations are not typically seen below 10 km — the appearance of this structure may point to the high signal-to-noise ratio that is achieved by the receiver equipment used on the COSMIC-2 satellites [2].

Figure 1.6 shows an estimated length-scale of the correlations shown in Figure 1.5. The length-scale is estimated by fitting a Gaussian distribution to each column of the correlation matrix. This accounts only for the positive core of the correlations, since the fitting function cannot be negative.

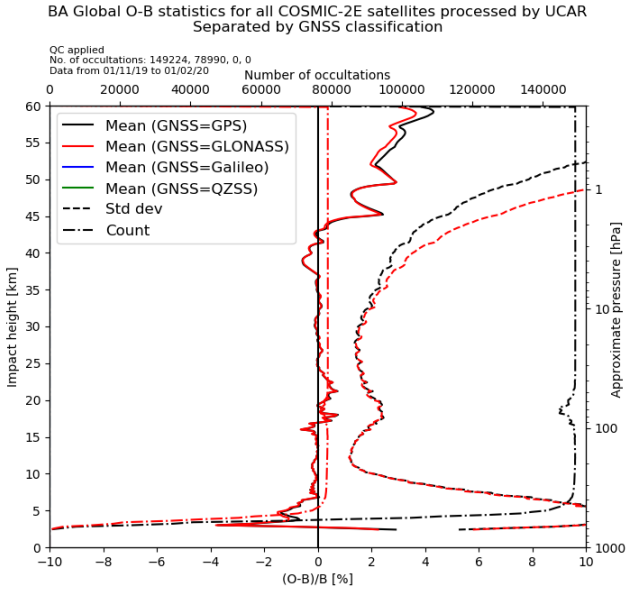

Figure 1.4: The bias and standard deviation of the normalised difference between the observation and the NWP model background forecast $(O-B)/B$ for bending angle, for different classes of GNSS with COSMIC-2.

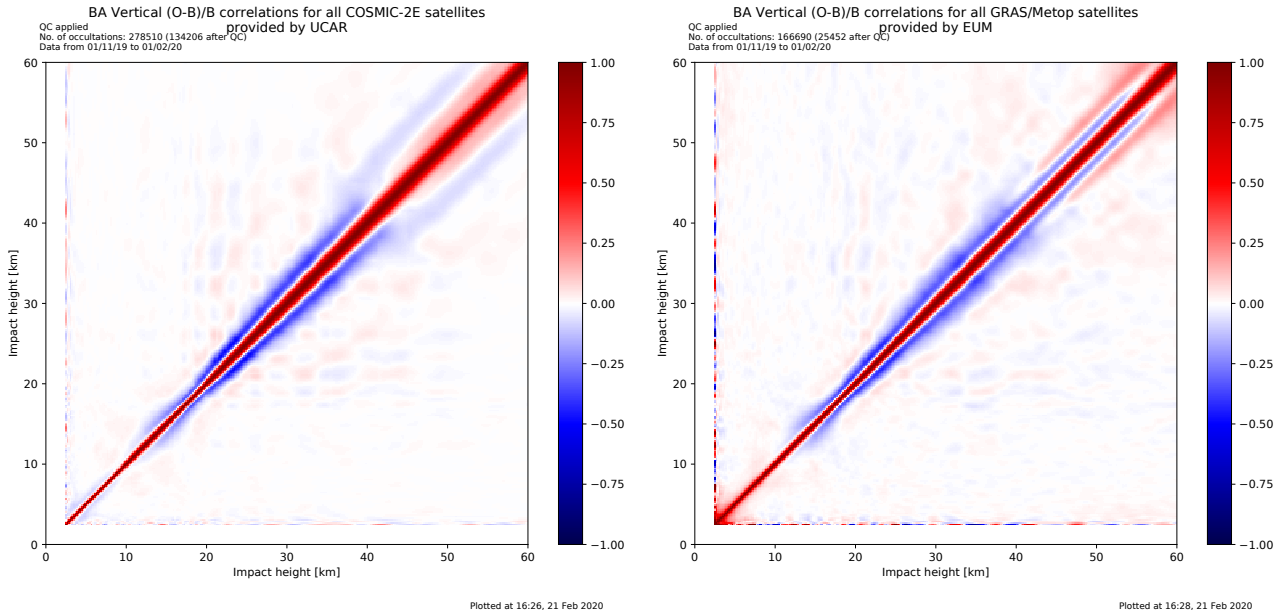

Figure 1.5: Vertical correlations of normalised differences between the observation and the NWP model background for bending angle. (left) Data from COSMIC-2 and (right) data from Metop.

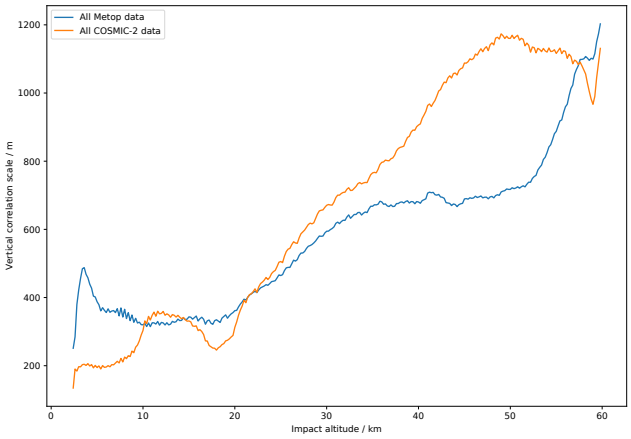

Figure 1.6: Estimated vertical correlation length scale as a function of height within the profile.

The reported length scale is the standard deviation of the fitted Gaussian. The vertical grid separation is 200m, so figures near this value should be treated with some caution. This highlights the increase of the vertical correlations for the Metop data in the troposphere. In the lower and mid-stratosphere the vertical correlations for COSMIC-2 are only slightly larger than those for the Metop satellites. This may mean that differences in vertical smoothing alone do not account for the differences in standard deviation seen in Figure 1.1

2 Refractivity statistics

Measurements of refractivity are calculated from the bending angle, using an Abel integral with assumptions about the spherical symmetry of the atmosphere. Figure 2.1 shows the mean and standard deviation of normalised differences between the observed refractivity and that produced by the NWP model forecast (i.e. the normalised innovations for refractivity). The mean normalised innovation is very similar for Metop and COSMIC-2 between 10 and 60 km. Below 10 km there are differences in the mean refractivity innovation, which is presumably related to the differences in the bending angle seen in this region. Above 40 km the standard deviation of the normalised innovation differs, with COSMIC-2 having larger standard deviations between 40 and 50 km, but smaller standard deviations above this. The behaviour between 40 and 50 km mimics the performance of the bending angles at high altitudes. Above this the differences will be due to the differences in climatology used by the two centres [1] and the weight given to this climatology in the statistical optimisation. Below 10 km the standard deviation of the innovation is lower for COSMIC-2 than for the Metop satellites. The COSMIC-2 receiver (TGRS) demonstrates a higher signal-to-noise ratio than instruments that have been used before [2], which should allow it to better resolve features in the troposphere. This may explain the better performance of the COSMIC-2 data in this region.

The vertical correlation of the difference between modelled and observed refractivity are shown in Figure 2.2 for COSMIC-2 and Metop. Since refractivity is derived from the vertical integral of the bending angles, it is expected that there are long-range correlations in this quantity. As with bending angle it is clear that the vertical correlation of refractivity is larger at high levels for COSMIC-2 than for Metop. There is also a region of substantial correlations between 10 and 20 km impact alitutude for COSMIC-2, which is not present in the Metop data. Below 10 km the correlations for COSMIC-2 are shorter range than for Metop.

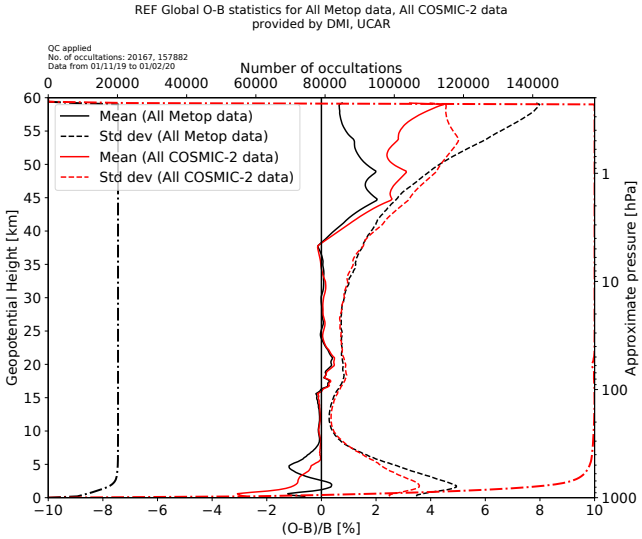

Figure 2.1: The bias and standard deviation of the normalised difference between the observation and the NWP model background forecast $(O-B)/B$ for refractivity.

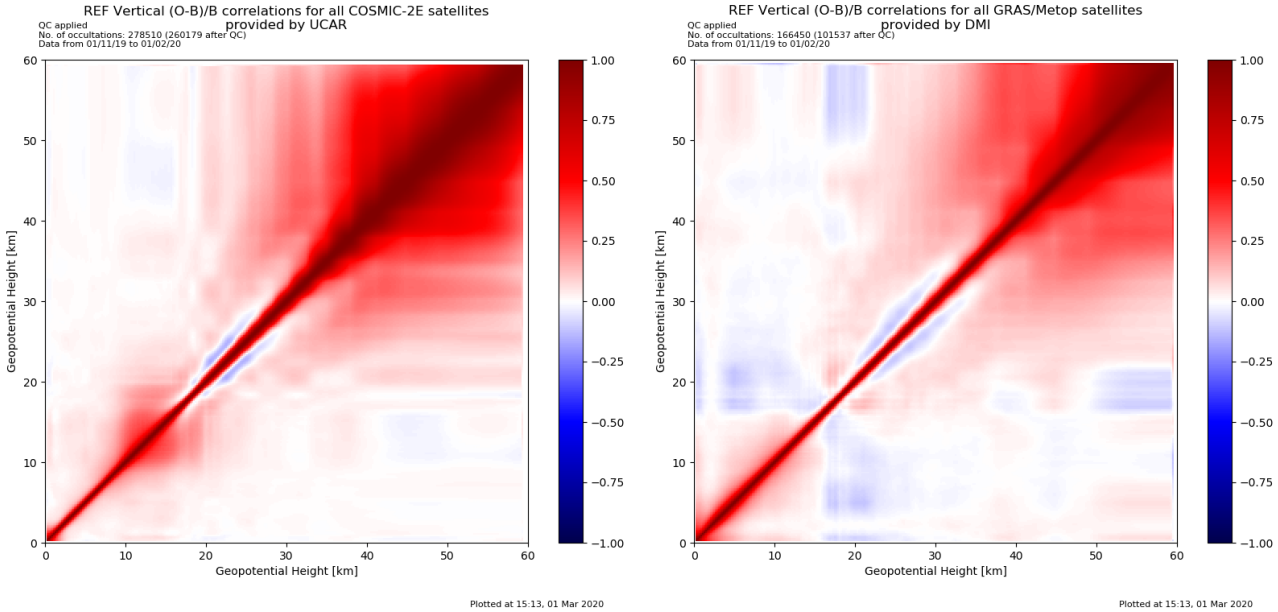

Figure 2.2: Vertical correlations of normalised differences between the observation and the NWP model background for refractivity, for COSMIC-2 (left) and Metop (right).

3 Tests within the assimilation system

In order to test the impact that adding these observations would have on the operational NWP system an assimilation test was run. This test mimics the operational system at low resolution, adding bending angle observations from the COSMIC-2 constellation to the data assimilation. This is compared with a similar low-resolution run without the additional observations. This control system includes observations from FY-3D and KOMPSAT-5, which were recently added to the operational system. There are three main factors that will mean that the impact estimated here is different from that which will be seen when the data becomes operationally available over the global telecommunications system (GTS):

- This test used offline data, therefore no account is made of the time that would be taken for the observations to arrive at the Met Office.
- Fewer observations have been made available through this testing period, with some satellites not producing observations for an extended period.
- Since the satellites were launched together they were initially located closely to each other. The process of the satellites spreading out is taking some time.

The second and third items will cause the impact to be under-estimated, and these are probably the dominant factors. Therefore, we expect that the benefit from assimilating COSMIC-2 observations operationally will be larger than the results shown here.

The test was run between 1st October 2019 and 31st January 2020 using a global forecast model at N320 resolution (640x480 grid-points). 7-day forecasts are launched every 12h, and these are verified against ECMWF analyses and against observations. Verification results are shown in Figure 3.1. There are substantial benefits for assimilating these observations. The largest benefits are for upper-level temperatures in the tropical region, but there are also reductions in the RMSE for winds in the tropics and temperature in the extra-tropics. The constellation provides data up to 47 degrees away from the equator, which drives the benefits to the NWP forecast in the extra-tropics.

When assessing forecast performance, we also consider assimilation statistics. This is the root-mean-square (RMS) difference between the forecast from the previous data assimilation cycle (6h ago) and the observations (i.e. the innovations for various observation types). There is a general reduction in the RMS innovation when assimilating observations from COSMIC-2 (not shown), indicating that these observations are making clear improvements to the quality of the analyses.

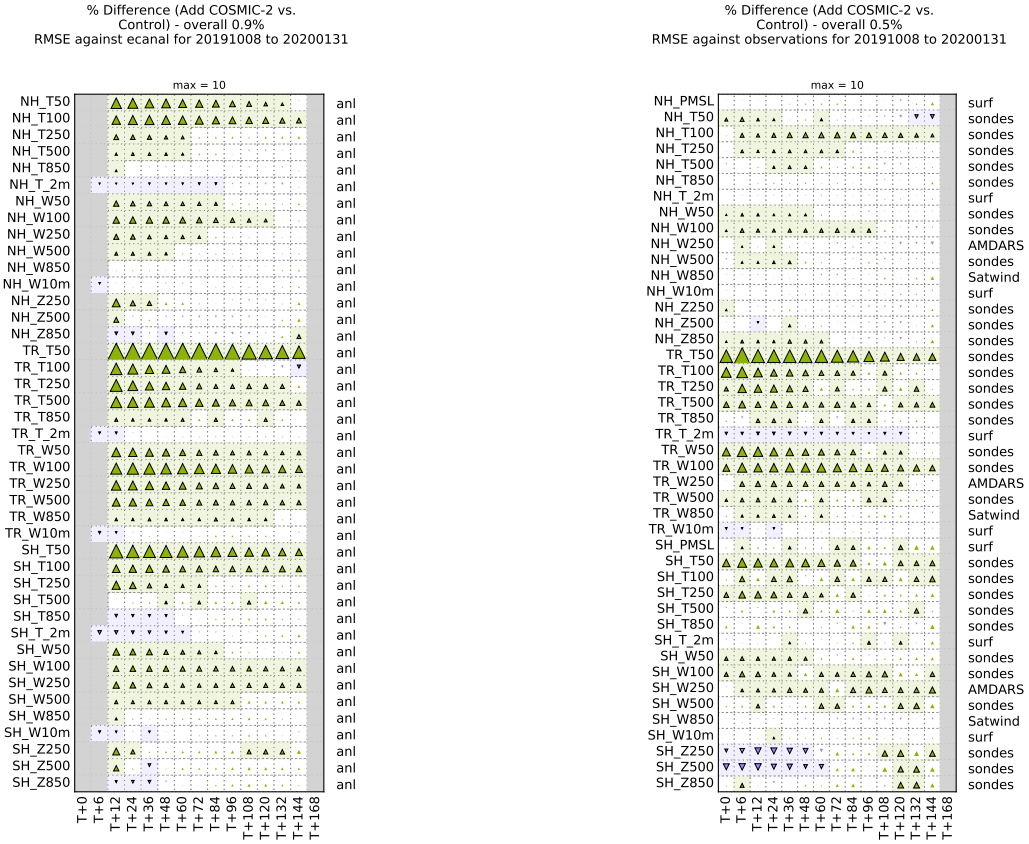

Figure 3.1: Verification results for a test using observations from COSMIC-2, compared to a baseline system. (left) Verification against ECMWF analyses and (right) verification against observations. The triangles show the change in the root-mean-square (RMS) error of the forecast, with green (blue) triangles indicating that the test has smaller (larger) errors. Where the change is statistically significant the box surrounding the triangle is shaded.

4 Separation of satellites

Since the satellites were all launched on a single rocket, they are gradually separating for each other. It is expected that they will be evenly spaced from each other by May 2021 [2]. Therefore the observations are currently more closely spaced to each other than would be desirable. It is interesting to understand the average inter-observation separation, as this affects the usefulness of the observations for NWP.

Figure 4.1 shows the distribution of occultation locations from COSMIC-2 between 9 and 15 UTC on 30th January 2020. This date was chosen as it corresponds to an assimilation cycle where observations from all six satellites are available. Most of the satellites are in similar orbits and the swath of observations provided by each overlaps with the others. The exception to this is COSMIC-2 E1, which was the first to descend to its final altitude of 550 km. As a consequence its observations are somewhat separate to the rest.

To further understand this, the separation between an observation and its closest neighbouring observation from a different satellite within a timespan of one hour was calculated. Figure 4.2 shows the frequency distribution of this minimum separation, calculated for the same set of observations as in Figure 4.1. This shows that many observations are separated by 100 km or less, although the majority have a much greater separation. Although thinning of the observations is applied to satellite radiance observations, the Met Office does not apply thinning to GNSS-RO observations. Therefore the results shown in Figure 3.1 will include these observations that are located close to each other.

Each of the six satellites in the COSMIC-2 constellation should provide data of the same quality as the other satellites. Figure 4.3 gives statistics for each of the six satellites. COSMIC-2 E4 and E6 provide many fewer observations than the other four satellites, which reflects that they have spent longer being removed from operations than the other satellites. Below 40 km all six satellites have very similar values for the mean ans standard deviation of the innovations. Above this level there are some differences, with COSMIC-2 E1 and E4 having larger standard deviations than the others.

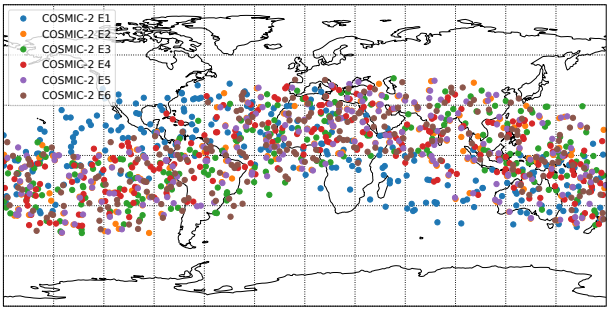

Figure 4.1: Occultation locations for observations made between 9 and 15 UTC on 30th January 2020.

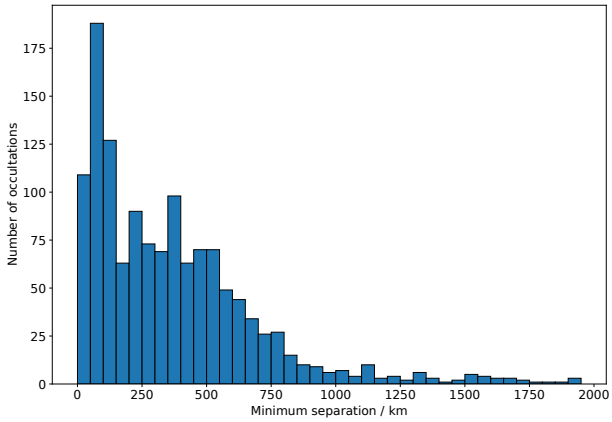

Figure 4.2: Distribution of the distance between an observation and its nearest neighbour, for observations taken less than an hour apart.

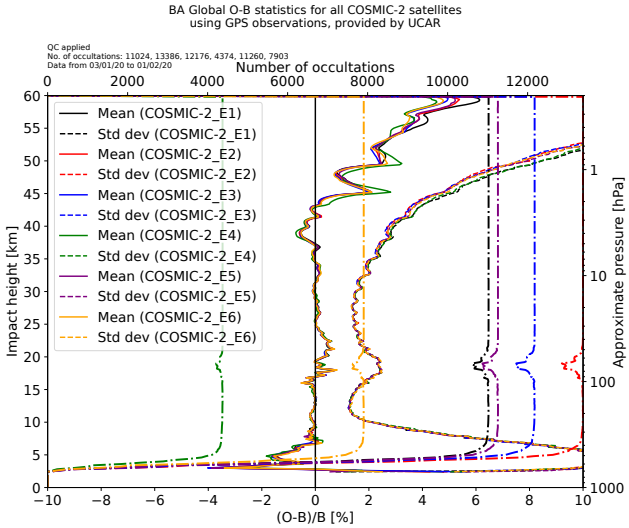

Figure 4.3: Mean and standard deviation of the bending angle innovation statistics, separated for each of the COSMIC-2 satellites.

5 Conclusion

This study has looked at observations from the COSMIC-2 constellation of satellites that are in a low-inclination orbit. It provides a large number of radio-occultation observations of high quality. There are a number of areas where these observations differ from those made by the Metop constellation of satellites.

- In some regions there are small differences in the bias of the bending angle between COSMIC-2 observations and those from Metop - above 50 km, below 10 km and between 17 and 20 km impact altitude.
- The standard deviations for bending angle are smaller for COSMIC-2 between 20 and 40 km. Above 40 km COSMIC-2 has larger standard deviations than Metop, and they are similar below 20 km.
- The vertical correlations of normalised bending angle innovation below 10 km have shorter length scales than those for Metop. There is evidence of negative correlations away from the diagonal, as is commonly seen above 20 km. This behaviour has not previously been observed for other satellite platforms.
- There are substantial benefits from assimilating the bending angles from COSMIC-2. These benefits are likely to increase as the satellites separate from each other, and as the data volumes become stable.

References

[1] M. E. Gorbunov and A. V. Shmakov. Statistically average atmospheric bending angle model based on COSMIC experimental data. *Izvestiya Atmospheric and Oceanic Physics*, 52:622–628, 2016.

[2] W.S. Schreiner, J.P. Weiss, R.A. Anthes, J. Braun, V. Chu, J. Fong, D. Hunt, Y.-H. Kuo, T. Meehan, W. Serafino, J. Sjoberg, S. Sokolovskiy, E. Talaat, T.K. Wee, and Z. Zeng. COSMIC-2 Radio Occultation Constellation: First Results. *Geophys Res Lett*, 47:1–7, 2020. doi: 10.1029/2019GL086841.

ROM SAF (and earlier GRAS SAF) Reports

SAF/GRAS/METO/REP/GSR/001	Mono-dimensional thinning for GPS Radio Occulation
SAF/GRAS/METO/REP/GSR/002	Geodesy calculations in ROPP
SAF/GRAS/METO/REP/GSR/003	ROPP minimiser - minROPP
SAF/GRAS/METO/REP/GSR/004	Error function calculation in ROPP
SAF/GRAS/METO/REP/GSR/005	Refractivity calculations in ROPP
SAF/GRAS/METO/REP/GSR/006	Levenberg-Marquardt minimisation in ROPP
SAF/GRAS/METO/REP/GSR/007	Abel integral calculations in ROPP
SAF/GRAS/METO/REP/GSR/008	ROPP thinner algorithm
SAF/GRAS/METO/REP/GSR/009	Refractivity coefficients used in the assimilation of GPS radio occultation measurements
SAF/GRAS/METO/REP/GSR/010	Latitudinal Binning and Area-Weighted Averaging of Irregularly Distributed Radio Occultation Data
SAF/GRAS/METO/REP/GSR/011	ROPP 1dVar validation
SAF/GRAS/METO/REP/GSR/012	Assimilation of Global Positioning System Radio Occultation Data in the ECMWF ERA-Interim Re-analysis
SAF/GRAS/METO/REP/GSR/013	ROPP PP validation
SAF/ROM/METO/REP/RSR/014	A review of the geodesy calculations in ROPP
SAF/ROM/METO/REP/RSR/015	Improvements to the ROPP refractivity and bending angle operators
SAF/ROM/METO/REP/RSR/016	Simplifying EGM96 undulation calculations in ROPP
SAF/ROM/METO/REP/RSR/017	Simulation of L1 and L2 bending angles with a model ionosphere
SAF/ROM/METO/REP/RSR/018	Single Frequency Radio Occultation Retrievals: Impact on Numerical Weather Prediction
SAF/ROM/METO/REP/RSR/019	Implementation of the ROPP two-dimensional bending angle observation operator in an NWP system
SAF/ROM/METO/REP/RSR/020	Interpolation artefact in ECMWF monthly standard deviation plots
SAF/ROM/METO/REP/RSR/021	5th ROM SAF User Workshop on Applications of GPS radio occultation measurements
SAF/ROM/METO/REP/RSR/022	The use of the GPS radio occultation reflection flag for NWP applications
SAF/ROM/METO/REP/RSR/023	Assessment of a potential reflection flag product
SAF/ROM/METO/REP/RSR/024	The calculation of planetary boundary layer heights in ROPP
SAF/ROM/METO/REP/RSR/025	Survey on user requirements for potential ionospheric products from EPS-SG radio occultation measurements

ROM SAF (and earlier GRAS SAF) Reports (cont.)

SAF/ROM/METO/REP/RSR/026	Estimates of GNSS radio occultation bending angle and refractivity error statistics
SAF/ROM/METO/REP/RSR/027	Recent forecast impact experiments with GPS radio occultation measurements
SAF/ROM/METO/REP/RSR/028	Description of wave optics modelling in ROPP-9 and suggested improvements for ROPP-9.1
SAF/ROM/METO/REP/RSR/029	Testing reprocessed GPS radio occultation datasets in a reanalysis system
SAF/ROM/METO/REP/RSR/030	A first look at the feasibility of assimilating single and dual frequency bending angles
SAF/ROM/METO/REP/RSR/031	Sensitivity of some RO measurements to the shape of the ionospheric electron density profile
SAF/ROM/METO/REP/RSR/032	An initial assessment of the quality of RO data from KOMPSAT-5
SAF/ROM/METO/REP/RSR/033	Some science changes in ROPP-9.1
SAF/ROM/METO/REP/RSR/034	An initial assessment of the quality of RO data from Metop-C
SAF/ROM/METO/REP/RSR/035	An initial assessment of the quality of RO data from FY-3D
SAF/ROM/METO/REP/RSR/036	An initial assessment of the quality of RO data from PAZ
SAF/ROM/METO/REP/RSR/037	6th ROM SAF User Workshop

ROM SAF Reports are accessible via the ROM SAF website: http://www.romsaf.org